AIAA 2004-4181

Improvements to the Linear Standard Stability Prediction Program (SSP)

J. C. French
Software and Engineering Associates
Carson City, NV 89701

G. A. Flandro and J. Majdalani
Advanced Theoretical Research Center
University of Tennessee Space Institute
Tullahoma, TN 37388

40th AIAA/ASME/SAE/ASEE Joint Propulsion Conference and Exhibit
11–14 July 2004
Fort Lauderdale, FL

40th AIAA / ASME / SAE / ASEE Joint Propulsion Conference and Exhibit **AIAA-2004-4181**
Broward County Convention Center
Fort Lauderdale, Florida
11-14 July 2004

IMPROVEMENTS TO THE LINEAR STANDARD STABILITY PREDICTION PROGRAM (SSP)

Jonathan French*, Software and Engineering Associates, Carson City, NV 89701
Gary Flandro† and Joseph Majdalani‡, University of Tennessee Space Institute, Tullahoma, TN 37388

ABSTRACT

Despite many decades of study, new solid rocket motors systems frequently experience unsteady gas motions and associated motor vibrations. This phenomenon most often occurs when the acoustic modes of the combustion chamber couple with combustion/flow processes. Current linear models of the sort used in the Standard Stability Prediction (SSP) code are designed to predict the tendency for a solid rocket motor to become unstable, but they do not provide any information on the *severity* of the instability (usually measured by the limit cycle amplitude of the oscillations) or on the *triggerability* (the tendency of an otherwise stable system to oscillate when pulsed with a sufficiently large disturbance) of the system. A goal of our present work is to build nonlinear capability into the the SSP tools. Success in incorporating useful nonlinear capabilities depends on a sufficiently complete and physically correct linear model. Accordingly, Software and Engineering Associates, Inc., has undertaken major improvements in the linear stability analysis and associated capabilities of the Solid Performance Program (SPP). These improvements support the development of new nonlinear capabilities to predict the oscillating pressure limit cycle amplitude, triggering and the DC pressure shift, the latter of which is often the most important threat to the rocket motor system resulting from combustion oscillations. In this paper, we focus on the recent additions and improvements to the linear SSP module. These include major improvement to the linkage between the rocket design code and SSP, and the inclusion of rotational flow effects that allow the satisfaction of key boundary conditions in the unsteady flow field solutions. The enhanced capability of the SSP is demonstrated by comparing the modified code to previous analyses for several solid rocket motors covering a wide range of typical design characteristics. Examples include systems predicted to be stable by earlier versions of the SSP code that were in fact inherently unstable. The improved linear code yields results which better fit the experimental findings.

INTRODUCTION

Solid rocket motor combustion instability occurs when combustion processes inside the rocket motor become coupled with the acoustic modes of the combustion chamber. While the Standard Stability Prediction program (SSP)[1] was developed to evaluate SRM stability, it can only predict if a motor might be unstable, as it is based on a linear stability analysis of the motor. Once a motor goes unstable, it can either explode or enter a limited amplitude pressure cycle, during which the pressure oscillates about a DC pressure shift. Prediction of the oscillatory pressure amplitude and the DC shift requires a nonlinear analysis of the interaction between the combustion processes and the acoustics of the combustion chamber.

The analytic approaches of Culick[2] and Flandro[3-4] for modeling combustion stability have been evaluated previously.[5] An underlying similarity between these approaches is their reliance on the linear stability analysis. If

* Jonathan French, Senior Research Engineer, Member AIAA
† Gary Flandro, Boling Chair Professor of Excellence in Propulsion, Department of Mechanical, Aerospace and Biomedical Engineering. Associate Fellow AIAA
‡ Joseph Majdalani, Jack D. Whitfield Professor of High Speed Flows, Department of Mechanical, Aerospace and Biomedical Engineering. Member AIAA

meaningful results are desired, an accurate evaluation of the linear stability analysis is required before attempting a nonlinear analysis. To this end, we have made several improvements to the linear stability analysis mechanism found in SSP, and revised the linear analysis itself to account for an improved understanding of the linear problem. In this paper, we review recent improvements to the SPP / SSP code set, and then apply several new stability integral sets by Flandro and Majdalani to both large and tactical solid rocket motors. In this section we demonstrate that SRMs may be less stable in the linear sense than has been previously assumed. The question remains as to how stable motors are in the nonlinear sense. Flandro explores this question in paper AIAA 2004-4182.[6]

In addition to these efforts, we have also sought to improve our multi-dimensional stability computation capability. SEA has previously developed both a 3D acoustic eigensolver and a 3D CFD code for use in combustion stability analysis. These codes have been limited to internal company use as 3D block volume grids had to be generated on a case by case basis due to the complexity of motor grain geometries. We considered incorporating a commercial package in order to provide our customers with a complete solution, but the cost was prohibitive. Instead, we have now developed our own grid generation code that uses the output of our solid rocket grain design and ballistics code, the Solid Performance Program (SPP) code, to generate volume grids. While the quality of the grids is not high and the cells may have collapsed corners or edges, the process is straightforward and only requires the user to input the maximum dimension of the cross-section of the computational domain (the axial dimension is chosen by the SPP input). The grid generation process and several sample cases are presented.

LINEAR STABILITY IMPROVEMENTS

The nonlinear combustion stability analysis is highly dependent on the accuracy of the linear stability analysis. In this section we present our improvements to the linear SSP code. The code itself has changed very little since its incorporation into SPP in 1987, and the fundamental underlying routines are robust. We have recently re-examined SSP, and the SPP/SSP linkage. These stability improvements are evaluated using the ASRM and Blomshield's Star-Aft motor.[7]

Geometry Resolution Improvements

The original SSP code required the user to specify the grain design and ballistics parameters manually for each web step under consideration. In 1987, SEA incorporated the SSP1D code into the SPP code, with the appropriate linkages to interpolate the SPP grain design and ballistics results onto 40 user-selected fixed axial locations. This did not allow the SSP code to track burning radial slot locations.

We have recently developed a new linkage which allows SSP to use the same axial stations specified by the user in SPP, so geometry and ballistics data are no longer interpolated from SPP to SSP. SPP contains a feature that allows it to reorder the axial station locations in order to track the radial slot motion as the slots burn back. These burning slot locations are now automatically passed to SSP. Also, SSP previously re-computed the internal steady flow velocity. SPP can now pass its computed steady axial velocity directly to SSP. As the nozzle damping stability term is linearly proportional to the mean velocity, this can have a significant effect on motor stability.

The exponential horn approximation, used to compute the acoustic mode shapes for axially varying cross-sections, is purported to be accurate as long as the area ratio between the ends of segment is less than a factor of two.[1] The perimeter is also approximated using the exponential horn relationship in order to yield analytic solutions to the surface stability integrals. To accommodate this limitation, if the areas are found to change too quickly across a segment, an additional axial station is inserted to split a single segment in two. The left segment and right segment areas are set to maintain a discontinuity at their interface. For example, for the rocket motor segment in Figure 1a, the cross sectional area changes too quickly. To accommodate the sudden area change, the segment is split in two and an additional axial station is inserted, as in Figure 1b. When the motor contains an axial slot, the insertion of the additional axial station correctly tracks the slot location.

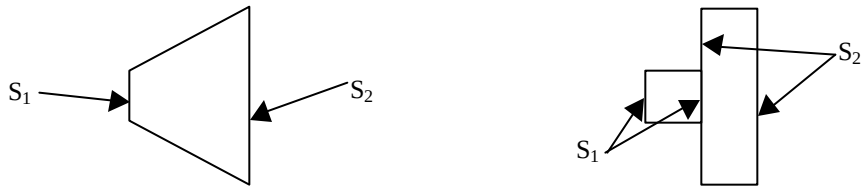

(a) Sudden change in cross-sectional area (S) (b) Substituted two discontinuous segments

Figure 1. Geometry Substitution for Sudden Expansions

Identification of Inhibited Surfaces

In SPP's V7 grain design input, to define the motor grain, the user first defines the motor case. It is assumed that the case is filled with grain. The user then specifies geometric shapes (ie cones, prisms, tori) or macros (ie star, dendrite, concocyl) that hollow out the grain, creating voids and defining burning surfaces. The shapes and macros all have a common parameter that allow the user to define the particular shape as non-burning – that is, the surface that shape hollows out will not grow with time. Normally, when a shape is allowed to burn, the amount of grain burned during a web step is computed via the difference in cross sectional areas between web steps. Thus, SPP does not need to explicitly compute the perimeter at each web step in order to compute the internal ballistics. SEA has written an additional algorithm that does determine the perimeter of the motor grain and internal surfaces at given axial locations. However, in the process of computing the perimeter, the information concerning whether or not a surface is inhibited is lost. In order to use this new perimeter computation in SSP, it was necessary to identify burning and non-burning surfaces, as most of SSP's stability integrals are surface integrals over the burning or non-burning surfaces.

In order to determine if a portion of the grid is inhibited, the perimeter computation is repeated at a web step slightly into the future. The new perimeter is compared with the previous computation. If a point on the perimeter does not move, that point is identified as being on an inhibited surface. For example, in Figure 2, the two radial slots are inhibited, and this grain feature is illustrated by plotting the identified inhibited surface in cyan (burning surfaces are red, and the exposed case is green). Previously, inhibited surfaces were incorrectly identified by the perimeter algorithm as burning surfaces, which in turn affected the stability computation for the new SPP / SSP linkage.

Implementation of Improvements

The ASRM test case grain design burn back is shown in Figure 2. The ASRM grain design consists of an 11-point star at the head end and two radial slots. We have used this motor to examine how our SPP and SSP improvements affected the computed stability, and have produced two sets of results. For the ASRM, the frequency computation was significantly affected by the improvements, shifting 10% from 12.75 Hz to 11.5 Hz during the first portion of the burn (Figure 3a). This is probably due to a much better resolution of the radial slots. The ASRM stability computation was not grossly affected. In contrast, for the small tactical motor, the frequency computation was similar between the new and old linkage approaches, but the stability analyses differ greatly (Figure 5). In this case, the difference in the stability is due to the nozzle damping term. The mean velocity at the exit to the nozzle in SPP was significantly different from that re-computed by SSP, due to erosive burning. Nozzle damping is linearly proportional to the mean exit velocity.

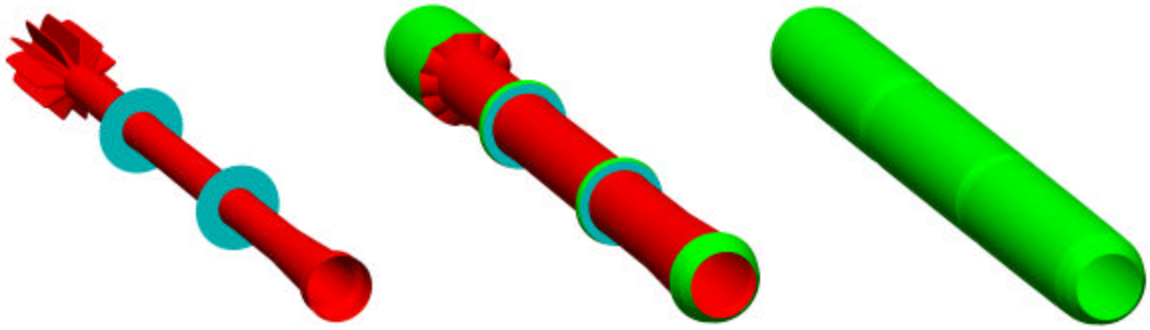

(a) Initial Grain Geometry (b) Mid-Burn (c) Fully Burnt

Figure 2. ASRM burn back at different time steps

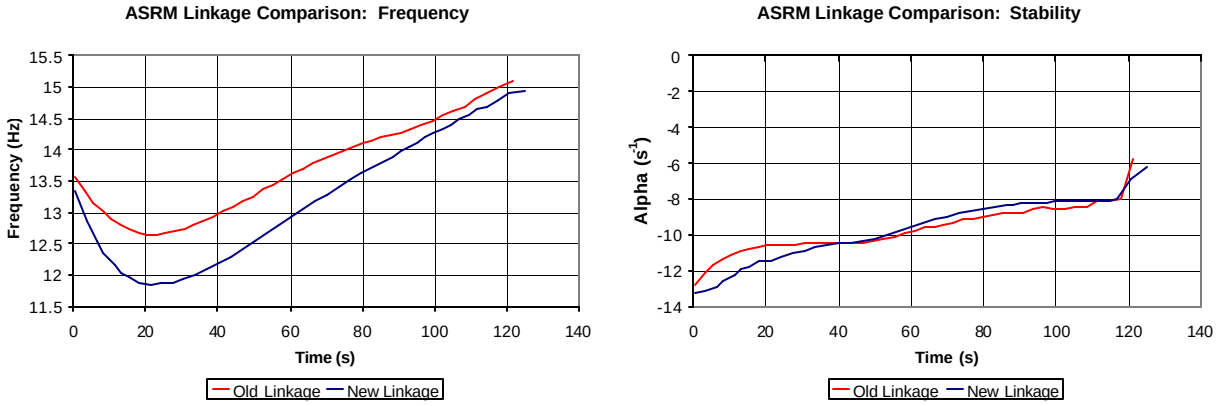

(a) Frequency (b) Stability

Figure 3. Improved SPP – SSP Linkage Effect on ASRM

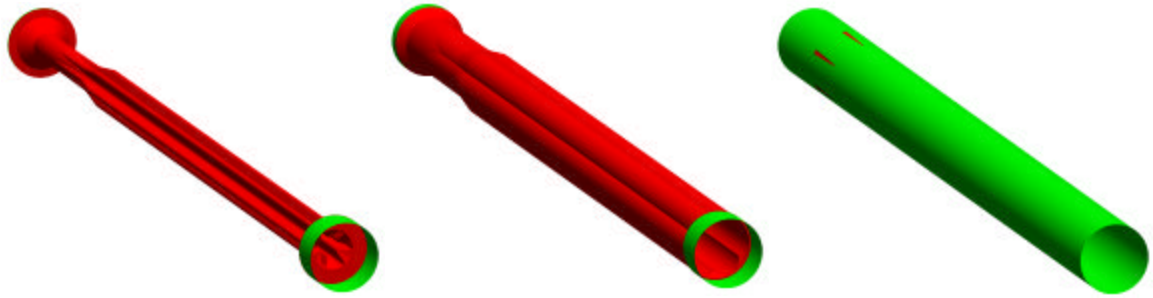

Figure 4. Burn Back of Blomshield's Star-Aft Motor

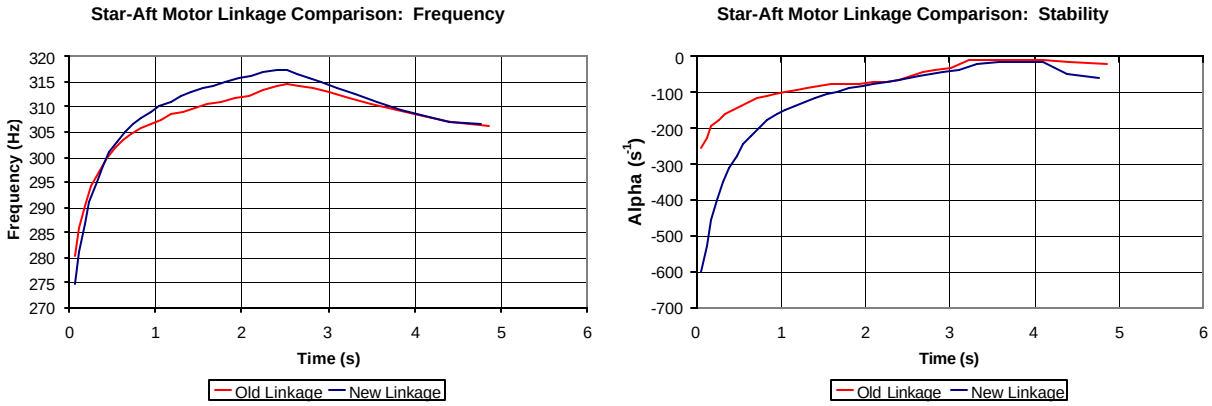

(a) Frequency (b) Stability

Figure 5. Improved SPP – SSP Linkage Effect on Blomshield's Star-Aft Motor

EVOLUTION OF LINEAR COMBUTION STABILITY METHODOLOGIES

The most daunting task of our nonlinear analysis effort has been to determine the underlying linear analysis. There is continued disagreement within the combustion stability community over which stability integrals should be included or excluded from the linear analysis, to say nothing of the nonlinear realm. Compounding the problem is experimental data. Experimentally measured results are technically nonlinear, making it difficult to evaluate the accuracy of the linear analysis. As a consequence, people may read into the results (experimental data and numeric computations) the answers they want to see or which past experience as led them to expect. From a managerial standpoint, it is greatly desirable to demonstrate that a SRM has a stable linear analysis, corresponding to a negative stability parameter. Recent derivations suggest that past analyses may have been too generous in their stability margin. It may turn out that motors are generally less stable in the linear analysis, but sufficiently stable when considered in a nonlinear analysis. In any case, the best proof as to which stability integrals are necessary would be the development of an associated nonlinear analysis that consistently predicts limiting amplitudes, DC shifts and triggering. The potential for such a development is presented in an associated paper.[6]

Analytic combustion stability theoretical modeling is difficult to verify experimentally, and there is considerable debate in how the boundary conditions should be treated. While SSP is often used to determine how motor modifications with affect the stability of a motor (increase or decrease stability), we need an absolute value in order to perform the nonlinear analysis. We have implemented the work of Gary Flandro, who has discovered several flaws in the original linear derivation. Corrections to each of these flaws have shifted the stability of SRMs in an undesirable direction towards decreased stability. Here is a brief overview of the theoretical evolution of Flandro and Majdalani's linear analysis:

1995 Flandro introduced a new rotational correction term in order to maintain the no-slip boundary condition for acoustic waves traveling parallel to burning surfaces.[8] He also eliminated the velocity coupling term. Velocity coupling presumes that the propellant combustion responds to the transverse acoustic velocity, in addition to responding to the pressure oscillations. The velocity coupling response is difficult to measure experimentally. Also, in light of the no-slip boundary condition, the perturbed transverse velocity at the burning surface is zero.

2003 Flandro and Majdalani introduced additional linear correction terms, including terms involving the pseudo-pressure, the pressure variation due to vortical waves.[9] The resulting new integrals were reduced to surface integral form, and evaluated for magnitude in comparison to M_b, the burning rate of the propellant. Two significant terms were identified: a vortical and a viscous correction. The vortical correction was notably exactly half the value of the flow turning integral, but the opposite sign.

2004 Flandro, while working on his nonlinear analysis, discovered that the initial set of equations used to derive the stability integrals had an irrotational assumption imposed.[6] When the full rotational equation was used, the flow turning term cancelled exactly with a different term. In addition, the Flandro / Majdalani vortical stability integral was eliminated. Flandro reformulated the stability integrals from the energy equation, which made it easier to evaluate the rotational terms in terms of scalars rather than vectors. The isentropic assumption was eliminated, and heat transfer and viscosity were incorporated.

To demonstrate the evolution of the linear analysis, we have incorporated all of Flandro and Majdalani's linear stability integrals, in surface integral form, into SSP. As with all of the stability integral terms in SSP, they may be used or "turned off" by the user's input. In order to demonstrate how the predicted stability of SRMs has changed over time, we have evaluated the stability of a large booster and a tactical motor (the ASRM and Blomshield's Star-Aft motor). We evaluated the stability of each motor several times, in each case varying the stability integrals used. For each motor we used the following stability integrals:

1) Original stability integrals (pressure coupling, flow turning, velocity coupling, nozzle damping, particle damping, wall damping).
2) Same as (1), except turned off explicit velocity coupling.
3) Same as (2), except added Flandro's rotational correction term (Flandro 1995).
4) Same as (3), except added Flandro & Majdalani's vortical and viscous correction terms (Flandro / Majdalani 2003)
5) Same as (4), except turned off flow turning and the vortical correction term (Flandro 2004)

The stability of each motor vs. burn time is plotted in Figure 6 and Figure 7. While the elimination of the velocity coupling term made each motor slightly more stable, the rest of the changes to the linear analyses predicted that both motors are less stable. The latest stability prediction goes so far as to predict that for several times during each motor's burn, there is a time during which each motor is linearly unstable. This brings up a question that has been thus far ignored – what are the true implications of a positive linear stability parameter? It may be that previously the linear analysis was overly damped, so when a motor only occasionally went unstable, SSP still predicted a stable stability prediction. Only a nonlinear analysis will reveal the nature of a positive stability parameter on solid rocket motor combustion.

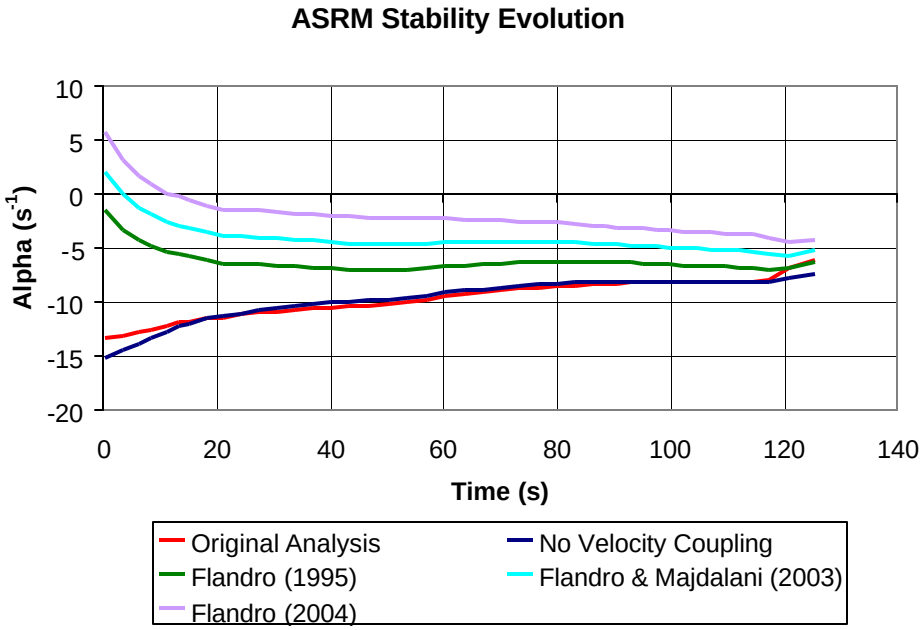

Figure 6. Application of Different Stability Integrals to ASRM

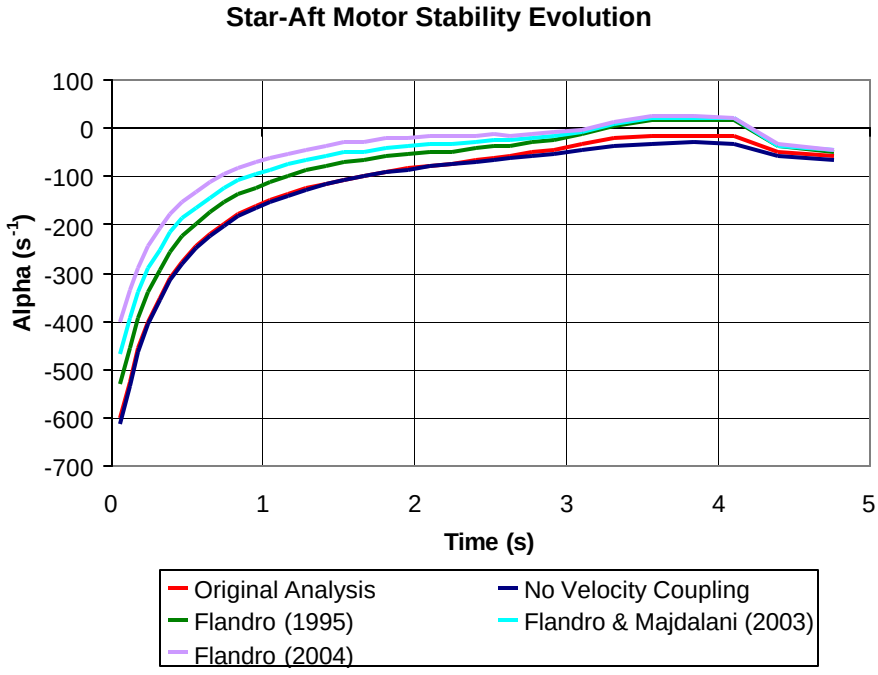

Figure 7. Application of Different Stability Integrals to Blomshield's Star-Aft Motor

3D GRID GENERATION

Using the SPP V7 grain design input format, SEA previously incorporated the ability to generate a finite element (FE) surface mesh of a solid rocket motor grain and non-burning surfaces.[10] SEA has also developed finite volume based CFD and acoustic eigensolver codes for combustion stability computations.[11] Implementation of the CFD and acoustics codes has been hampered by the lack of an automated and reliable tool that can generate a volume grid of the SRM void volume. SEA did develop a grid generation tool that created 2D grids based on each axial location's perimeter. Each 2D grid had the same dimensions at each axial station. A 3D grid was formed by attaching the adjacent 2D grids. If the motor geometry did not vary suddenly in the axial direction, a reasonable mesh was generated.[12] However, for motors with sudden axial changes in geometry such as radial slots, the resulting grids contained cells that were unreasonably stretched. Commercial grid generation codes were considered, but were too costly and did not provide for the level of automation desired. To facilitate steady and perturbed flow analyses, a grid generation tool was needed that could create volume grids for complicated geometries with a minimum of user input. To simplify the grid requirements, both our CFD and acoustics codes allow for blocks of structured Cartesian grids with collapsed nodes and edges, as both use the finite volume discretization approach.

Recently, we pursued an unconventional approach that appears to yield volume grids with minimal user intervention. While it should be noted from the start that the quality of the meshes generated using this technique is not high, the acoustics code appears to work well with the resulting mesh. Our main concern was to be able to capture sudden changes in geometry with a set of structured blocks of grids. The grids had to communicate at common boundary nodes without interpolation.

Our current process:

1. Transform the surface mesh (generated by SPP) into either ZRT space or a new XYZ space. The ZRT space transform yields a final grid that has nodes that converge at the centerline. The new XYZ space would transform one symmetry section plane to Y=0, and the other symmetry plane to Z=0, placing only a corner of the final grid along the centerline. We are currently working with the ZRT transform (Figure 8).
2. Cover the surface mesh with a Cartesian grid with the same overall dimensions (Figure 9). The Cartesian grid's number of axial nodes and their spatial locations match the SPP specified locations. The spatial dimensions of the cross-sectional plane is computed using the maximum values for the given motor. The user defines the actual number of nodes used in the cross-section of the Cartesian grid.
3. Identify both the grid nodes that are inside the mesh, and the grid nodes on the outside of the mesh that are next to grid nodes that are inside the mesh (Figure 10).
4. Shift the outside nodes next to mesh to the nearest mesh line within the same axial plane (Figure 11).
5. Shift the grid nodes to eliminate concave cells and to smooth surfaces between axial planes where the number of inside / outside nodes changes between axial planes (Figure 12).
6. Rotate the grid back to the original XYZ coordinate system (Figure 13)

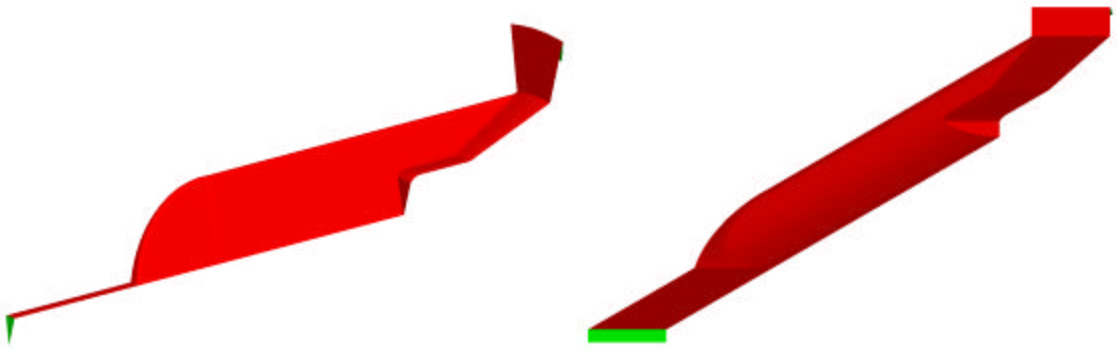

(a) XYZ (b) ZRT

Figure 8. Extended Delta Motor Surface Mesh

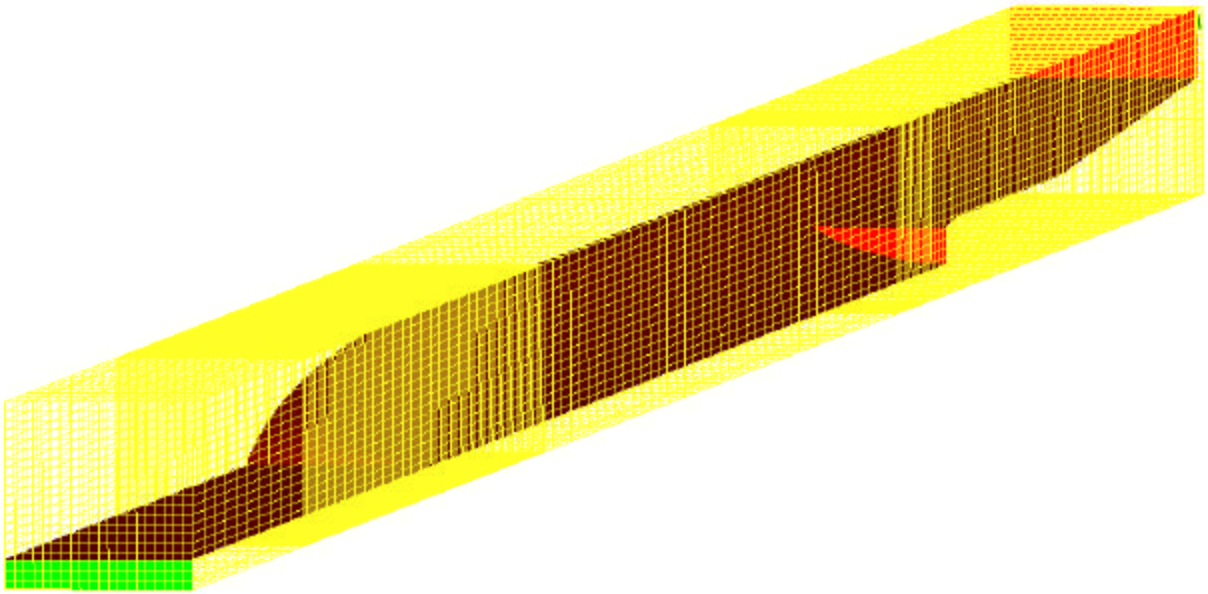

Figure 9. Surface Mesh Embedded in Cartesian Grid

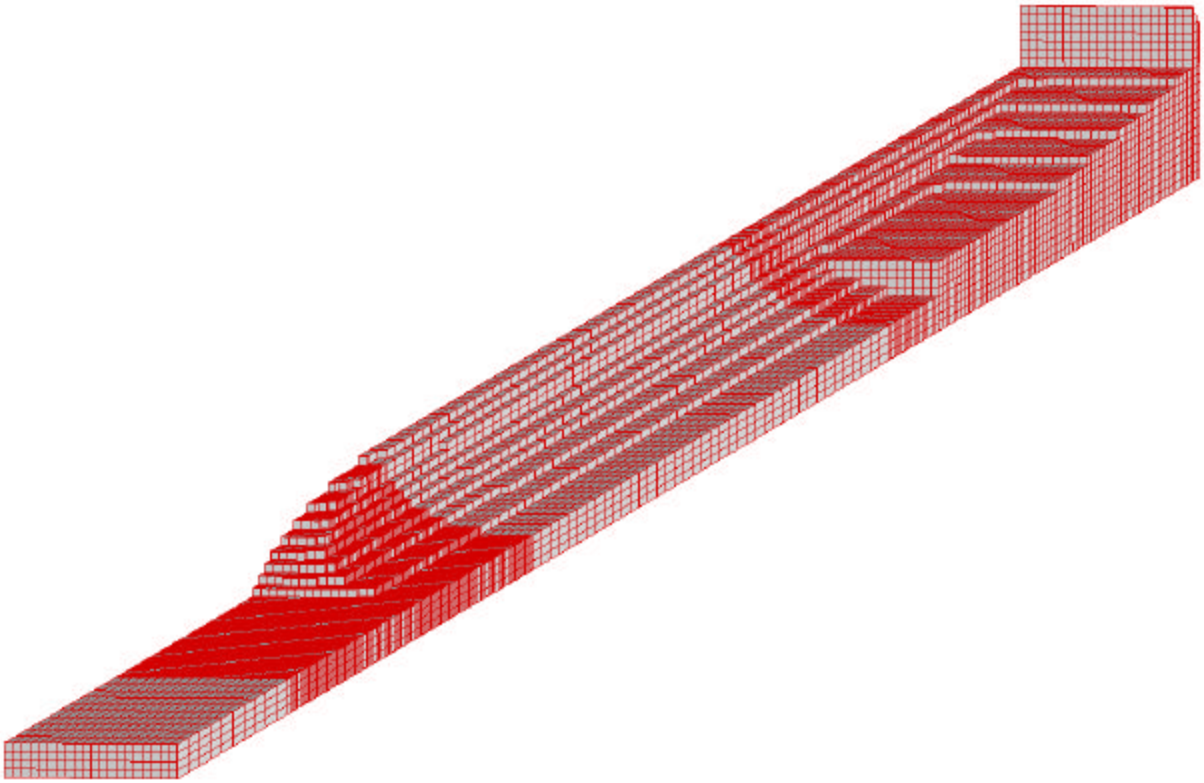

Figure 10. Grid Nodes Inside or Just Outside Surface Mesh

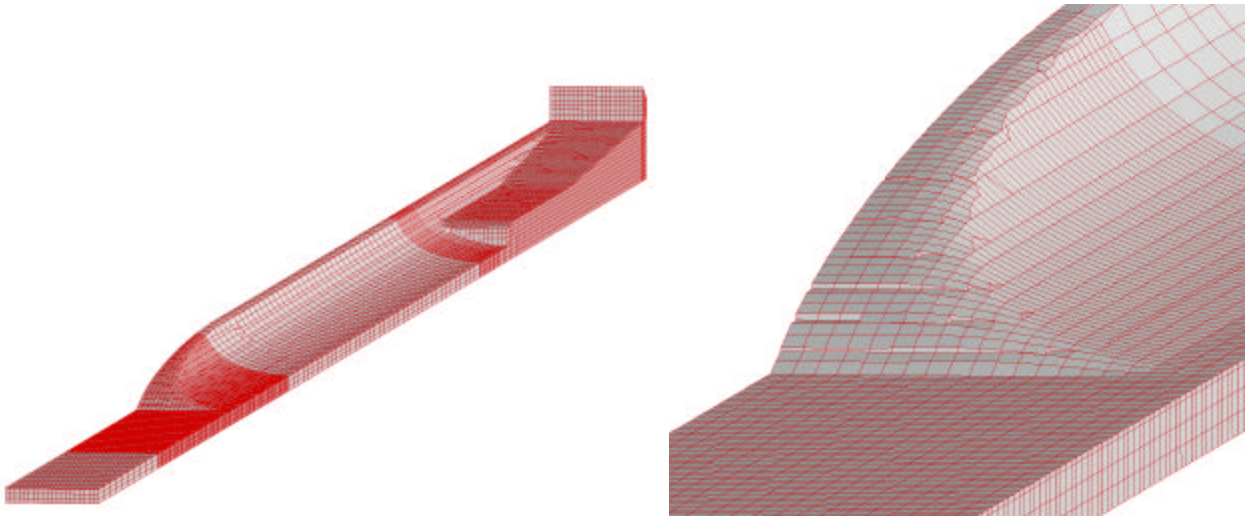

(a) Full Grid (b) Close-Up of Rough Region

Figure 11. “Rough” Grid

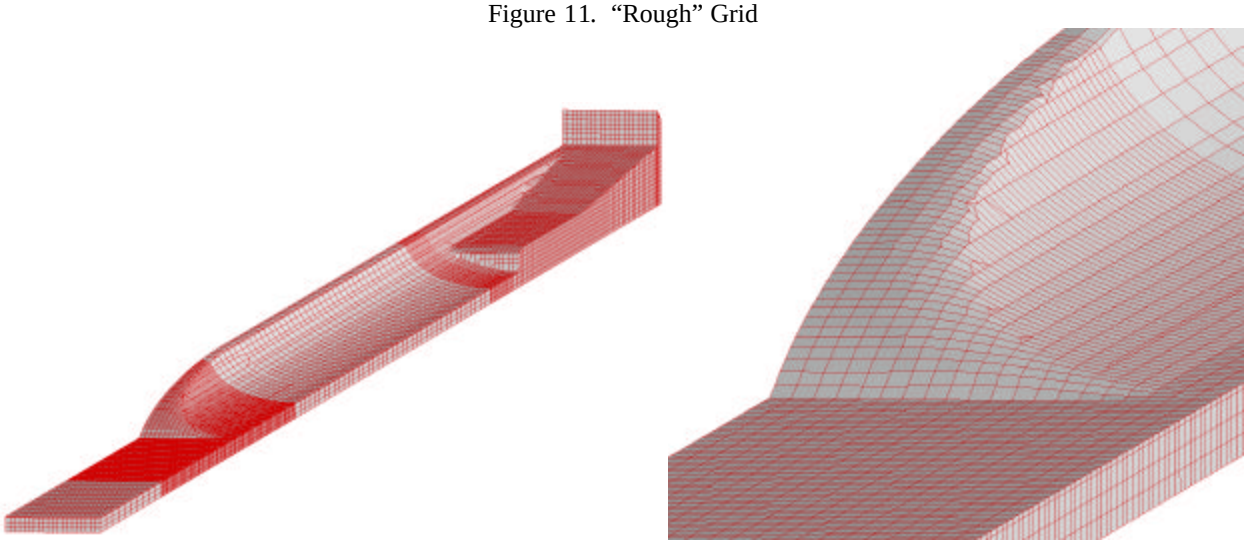

(a) Full Grid (b) Close-Up of Smooth Region

Figure 12. “Smooth” Grid

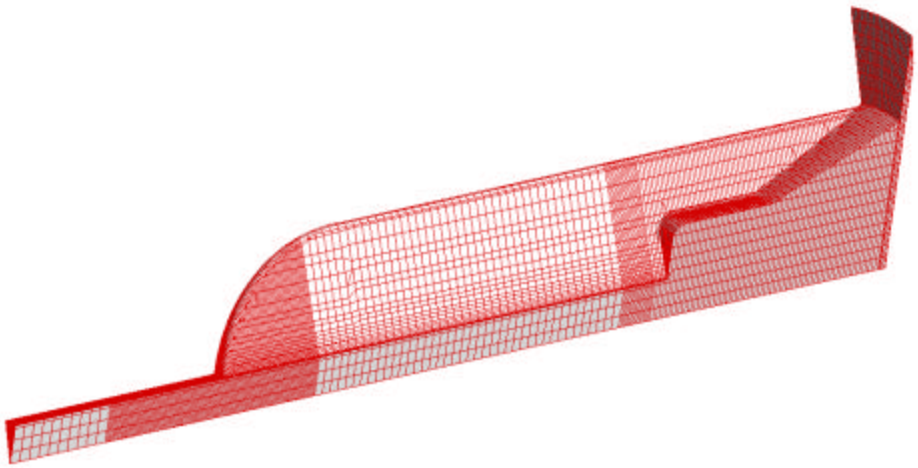

Figure 13. Final Grid (XYZ)

The resulting grid is "value blanked", with unused cells in the grid ignored in computations. This allows us to evaluate the grids using our acoustics code. As our CFD code does not allow for value blanking, we wrote an additional code to subdivide the value blanked grid into a series of smaller, attached blocks of grids, only utilizing the grid nodes that are not blanked. For a single symmetry section of the extended Delta motor, this yielded 14 blocks of grids. When the full motor is evaluated (such as for tangential mode acoustics), the value blanked grid is mirrored and rotated SYMFAC times to obtain the full motor geometry. When the grid blocks are rotated, this results in {SYMFAC * # of blocks of grids} grids. For the Extended delta motor, SYMFAC = 16, so the value blanking approach yielded 16 grids (see Figure 14a), and subdivision of the blocks of grids yielded (14 x 16 =) 224 grids (see Figure 14b). Subdivision of the grids allows for future parallelization of the acoustics and CFD codes.

At present, we have only used the generated grids with our acoustics code, as the grid generation code automatically generates the boundary condition input for the acoustics code. We are currently working on an automated CFD boundary condition code.

While we are still evaluating the results for accuracy, we have generated computational grids for the Extended Delta motor, generic double conocyl and dendrite grain designs, and Blomshield's Star-Aft motor[7]. For the Extended Delta motor, we have included here the 7^{th} axial mode and the 4^{th} tangential 1^{st} axial mixed mode results (Figure 15), computed using the blocks of grids shown in Figure 14b. The color contours are the perturbed pressure levels. The black lines are contour lines plotted on the surface where the perturbed pressure is zero, and thus represent pressure node locations. In the 7^{th} axial mode plot, the aft axial node line is swept into the aft end of the motor, due to the larger cross sectional area at the aft end of the motor.

We included several additional computations for the double conocyl and the dendrite grain designs. These computations demonstrate the non-axial nature of the acoustics at higher frequencies. The conocyl mode shapes show that the acoustic waves are truly 3D, and penetrate into the crevasses of the motor (Figure 17b, Figure 18 and Figure 19). The dendrite grid demonstrates that the grid generation technique can create a grid that smoothly transitions from a complicated dendrite geometry into a sudden axial expansion. At the interface, the nodes are stretched, but not in an unreasonable fashion (Figure 20a). The dendrite yielded several modes that do not fit the typical axial – tangential – radial designations (see Figure 20c and Figure 20d).

To demonstrate the flexability of the acoustics code, rather than evaluate the full set of mirrored and rotated grids, only the symmetry section grids of Blomshield's Star-Aft motor were used in this acoustics computation. The computation yields the axial and radial modes (and non-physical tangential modes). We have included the 4^{th} axial mode in Figure 21b. For demonstration purposes, we have also included the grids generated for later times during the burn (Figure 21c-d)

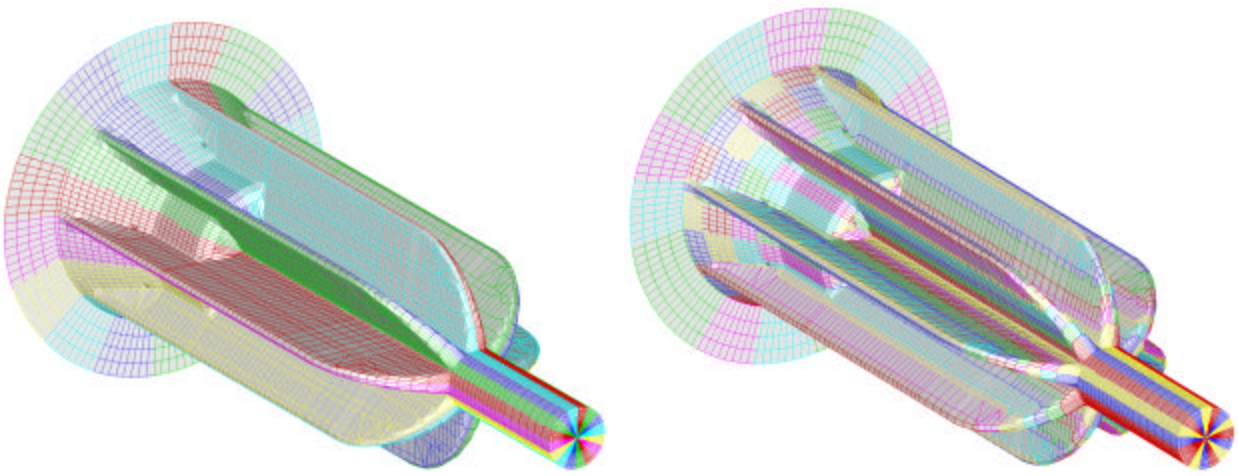

(a) Value Blanked (b) Subdivided Into Blocks

Figure 14. Extended Delta Motor

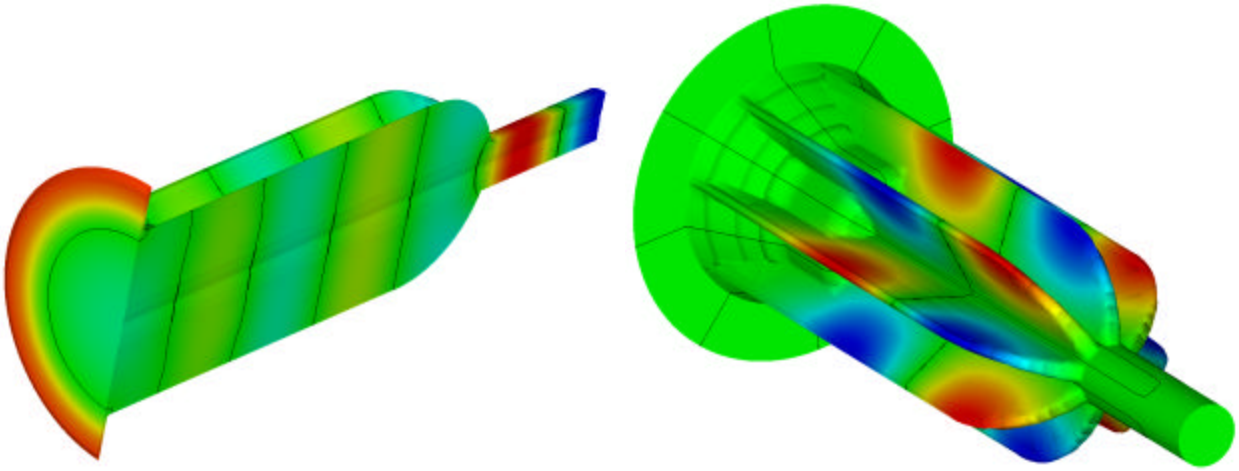

(a) 7th Axial Mode

1st Axial 4th Tangential Mode

Figure 15. Extended Delta Motor Acoustics

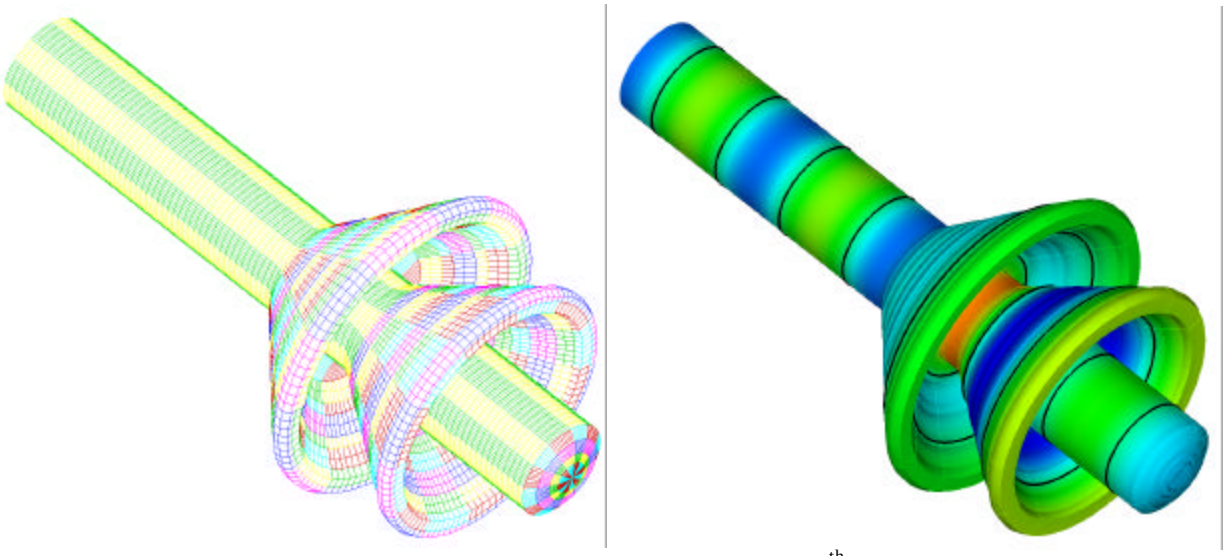

(a) Grid

(b) 8th Axial Mode

Figure 16. Conocyl

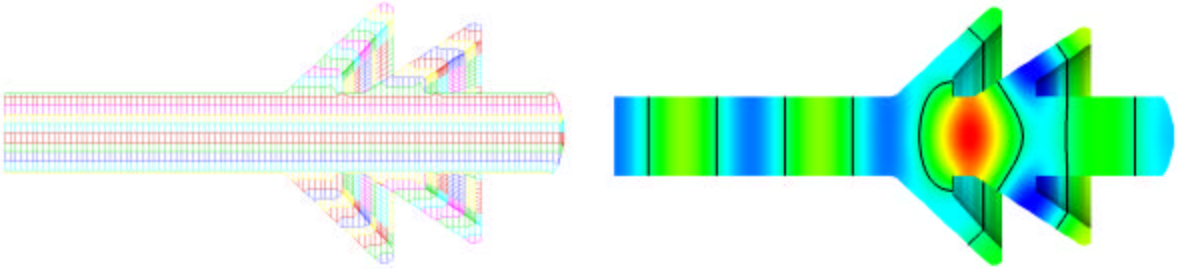

(a) Grid

(b) 8th Axial Mode

Figure 17. Conocyl (cross section)

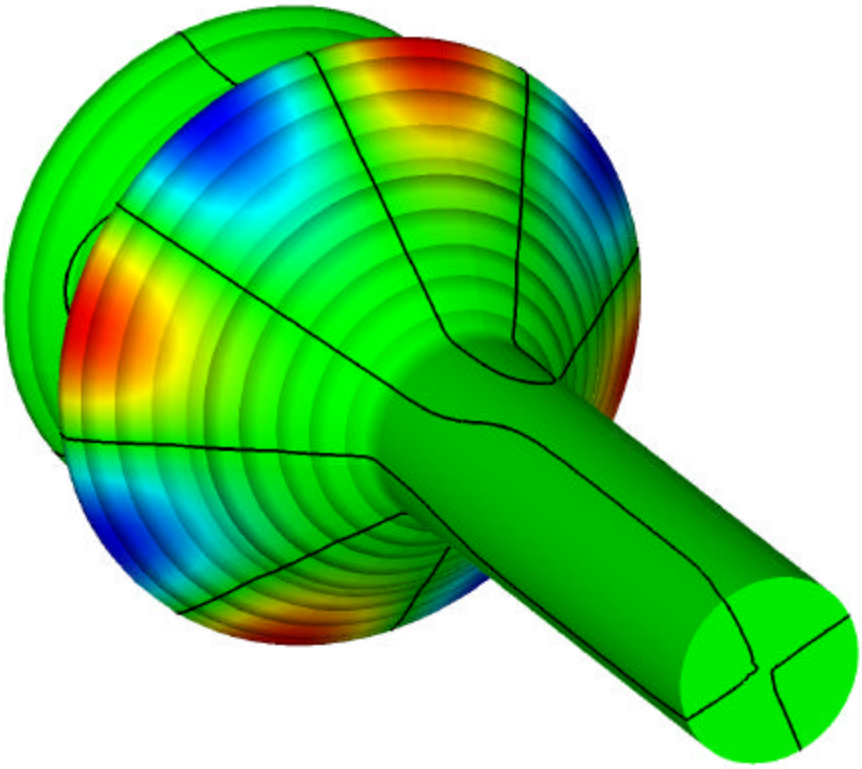

Figure 18. Conocyl 4th Tangential Mode

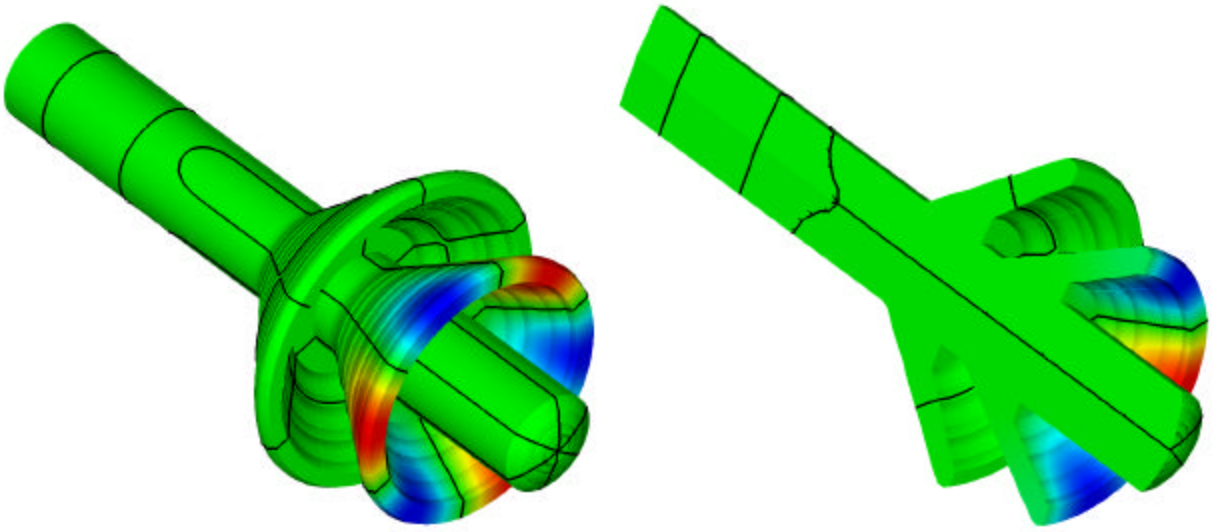

(a) 3rd Axial 3rd Tangential Mode (b) Cross Section

Figure 19. Conocyl Mixed Mode

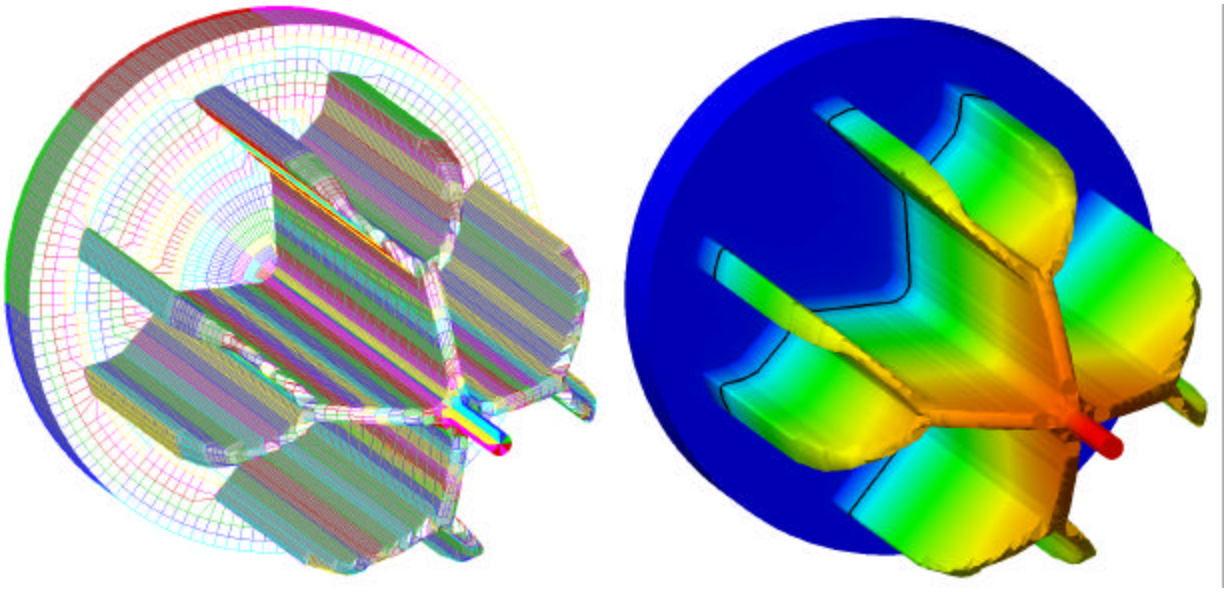

(a). Grid (b) First Axial Mode

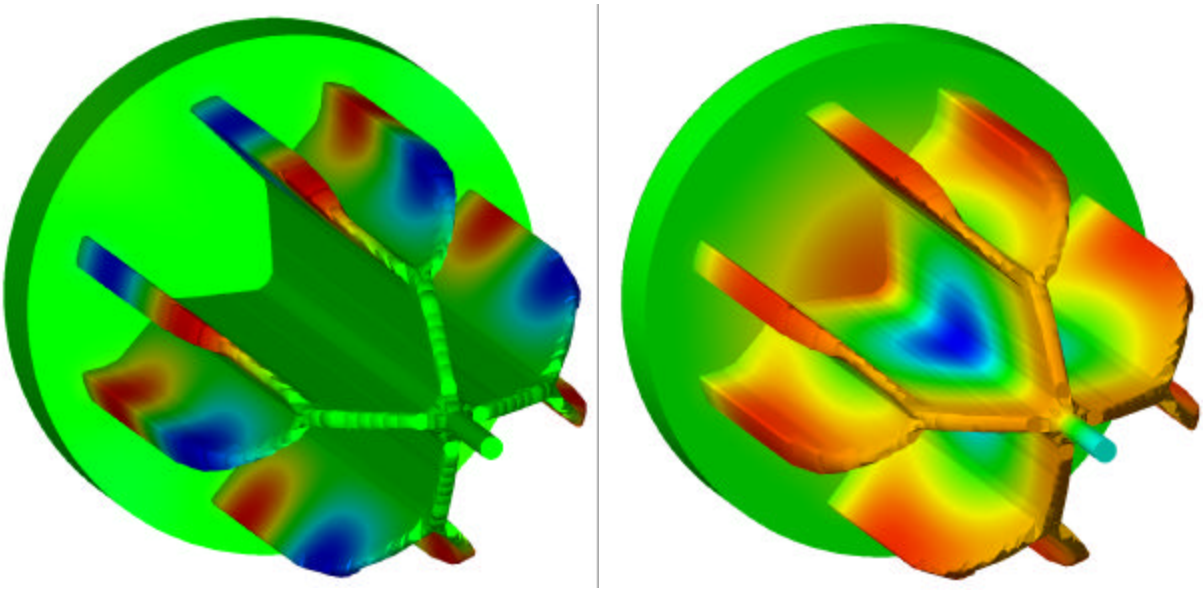

(c) Tangential Mode in Spokes (d) Radial Mode ?

Figure 20. Dendrite

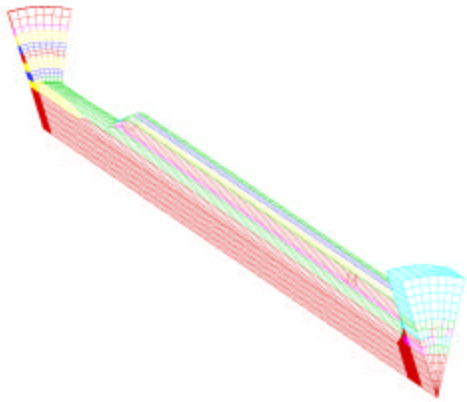

(a) Initial Grid (21 blocks)

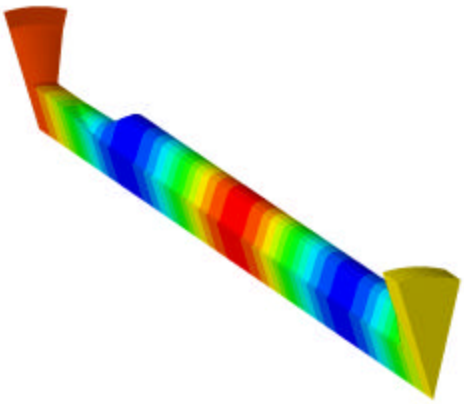

(b) Initial Grid's 4th Axial Mode

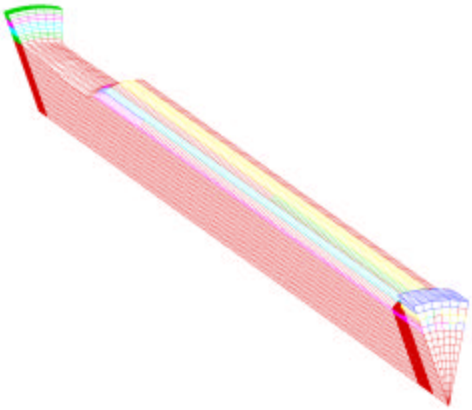

(b) Mid-Burn Grid (19 blocks)

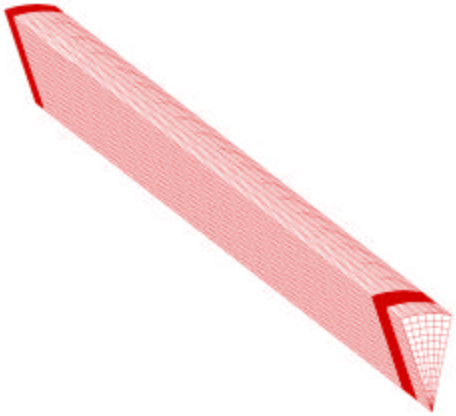

(c) Tail-Off Grid (1 block)

Figure 21. Blomshield's Star-Aft Motor

CONCLUSIONS AND FUTURE WORK

The SSP computations have been greatly improved by increasing the resolution of motor geometry, computation of an improved perimeter, passing the axial mean velocity from SPP directly (rather than computing it in SSP), and by identifying non-burning surfaces.

We have implemented Flandro and Majdalani's latest combustion stability theories into SSP, and noted that they imply that solid rocket motors are much less stable than previously thought. SEA is planning to implement Flandro's new nonlinear combustion stability analysis as a module of SPP. This new approach is designed to predict limiting amplitudes, triggering and the DC shift, coupling the slowly varying mean flow parameters to the stability analysis. We plan to compare the computed results with experimental data, and to re-evaluate response function data using a similar nonlinear technique. We prefer analytic to CFD approaches, as our codes are all designed to run quickly, within our end-user's design cycle.

Our new grid generation tool (designed to create structured volume grids, subdivided into fully connected blocks) appears to be robust. We plan to perform parametric studies to determine the relative quality of the grids, and also test the grids in conjunction with our CFD code.

ACKNOWLEDGEMENTS

We would first like to thank Fred Blomshield, of NAWC / China Lake, for his support in funding this effort. We appreciate the ongoing collaboration with Gary Flandro in deriving a reasonable yet out-of-the-box approach to nonlinear combustion stability modeling. Finally, we appreciate Joseph Majdalani's efforts to validate and verify our physical analyses and mathematical derivations before they appear in print.

[1] Nickerson, G.R., Culick, F.E.C., Dang, A.L., "The Solid Propellant Rocket Motor Performance Prediction Computer Program (SPP), Version 6.0, Volume VI: Standard Stability Prediction Method for Solid Rocket Motors, Axial Mode Computer Program User's Manual", Software and Engineering Associates, Inc., Carson City, NV 1976.

[2] Culick, F.E.C., and Yang, V., "Prediction of the Stability of Unsteady Motions in Solid Propellant Rocket Motors", Chapter 18 in *Nonsteady Burning and Combustion Stability of Solid Propellants*, Progress in Astronautics and Aeronautics, Vol. 143, 1992.

[3] Flandro, G.A., "Approximate Analysis of Nonlinear Instability with Shock Waves", AIAA-82-1220, 18th Joint Propulsion Conference, Cleveland, OH, June 1982.

[4] Flandro, G.A., "Energy Balance Analysis of Nonlinear Combustion Stability", *Journal of Propulsion and Power*, Vol 1, No 3, pp 210-221, May-June 1985.

[5] French, J.C., Flandro, G.A., "Nonlinear Combustion Stability Prediction with SPP/SSP", 39th JANNAF Combustion Subcommittee, Colorado Springs, CO, December 2003.

[6] Flandro G., French, J., Majdalani, J., "Incorporation of Nonlinear Capabilities in the Standard Stability Prediction Program", AIAA-2004-4182, 40th AIAA / ASME / SAE / ASEE Joint Propulsion Conference, Ft. Lauderdale, FL, July 2004.

[7] Blomshield, F.S., Stalnaker, R.A., "Pulsed Motor Firings: Pulse Amplitude, Formulation, and Enhanced Instrumentation", AIAA-98-3557, 34th AIAA Joint Propulsion Conference and Exhibit, Cleveland, OH, July 1998.

[8] Flandro, G.A., "Effects of Vorticity on Rocket Combustion Stability," *Journal of Propulsion and Power*, 1995, vol 11(4).

[9] Fischbach, S.R., Flandro, G.A., Majdalani, J., "Volume-to-Surface Transformations of Rocket Stability Integrals", AIAA 2004-4054, 40th AIAA / ASME / SAE / ASEE Joint Propulsion Conference, Ft. Lauderdale, FL, July 2004.

[10] French, J.C. and Dunn, S.S., "New Capabilities in Solid Rocket Motor Grain Design Modeling (SPP'02)", 38th JANNAF Combustion Subcommittee, Destin, FL, 2002.

[11] French, J.C., "Tangential Mode Instability of SRMs with Even and Odd Numbers of Slots", 38th AIAA / ASME / SAE / ASEE Joint Propulsion Conference, AIAA paper 2002-3612, Indianapolis, IN, July 2002.

[12] French, J.C., Coats, D.E., "Automated 3-D Solid Rocket Combustion Stability Analysis", 35th AIAA / ASME / SAE / ASEE Joint Propulsion Conference and Exhibit, Los Angeles, CA, AIAA 1999-2797.